



Structural Optimization of External Rotor Permanent Magnet Motor Based on Halbach Magnetization

Zhiyuan Ren, Tianyun Liu*

Institute of Nuclear and New Energy Technology, Tsinghua University, Beijing, China

Email address:

renzy22@mails.tsinghua.edu.cn (Zhiyuan Ren), liu-ty22@mails.tsinghua.edu.cn (Tianyun Liu)

*Corresponding author

To cite this article:

Zhiyuan Ren, Tianyun Liu. Structural Optimization of External Rotor Permanent Magnet Motor Based on Halbach Magnetization. *American Journal of Electrical Power and Energy Systems*. Vol. 12, No. 3, 2023, pp. 51-58. doi: 10.11648/j.epes.20231203.12

Received: June 14, 2023; **Accepted:** June 29, 2023; **Published:** July 6, 2023

Abstract: This paper takes an external rotor permanent magnet synchronous motor (ERPMM) as the research object, and analyzes the magnetic circuit structure and working principle of the motor. According to the design parameters and design structure of the motor, the motor is analyzed by combining the finite element method and the analytical method. In this paper, increasing the output torque of the motor and reducing the cogging torque are the optimization goals, and the design uses the Halbach magnetization structure as the main method to optimize the design of the motor to form an A-type Halbach magnetized external rotor permanent magnet motor (HERPMMMA). On the basis of improving the magnetizing structure, the structure of the permanent magnet motor is parametrically analyzed and optimally designed to form a B-type Halbach magnetized external rotor permanent magnet motor (HERPMMB). In this way, the torque performance of the motor can be further improved on the basis of giving full play to the advantages of Halbach's magnetization structure. The operating performance of the three motors is compared and analyzed, and the optimization results are evaluated by integrating multiple optimization objectives. The results show that the output torque and permanent magnet utilization of HERPMMB increased by 42.88%, and the cogging torque of the motor decreased by 78.63% compared with ERPMM without changing the amount of permanent magnets.

Keywords: Permanent Magnet Motor, Halbach Magnetization, Cogging Torque, Torque Output, Structural Optimization

1. Introduction

Permanent magnet motor has become a necessity in modern society due to its high power density, reliable structural design, low operating failure rate, stable operating performance, energy saving and high efficiency, and plays an important role in different application scenarios [1]. Especially in recent years, with the rise of new energy vehicles, motors have been more widely used and put forward higher requirements for various operating parameters [2, 3]. In the control rod drive mechanism of the high temperature gas-cooled reactor, the permanent magnet motor also plays the role of driving the movement of the control rods and buffering the speed of the falling rods [4].

The Halbach array is a permanent magnet array structure proposed by the American scholar Mallianson, which aims to provide a stronger magnetic field with fewer permanent magnets. The Halbach permanent magnet array directs the

magnetic field to the air gap on one side to show the characteristics of magnetic concentration, and has a good application in linear motors [5]. Kai Liu et al. [6] shows that the Halbach array can achieve higher air gap flux density and better sinusoidal air gap flux density, so that the output torque of the motor is higher and the torque ripple is lower. Wang Xiuping et al. [7] applied the Halbach array to the permanent magnet motor and added permanent magnets in the modulation cogging, which improved the utilization rate of the permanent magnets and reduced the no-load cogging torque. Xintong Zhang et al. [8] proposed a trapezoidal permanent magnet Halbach array, which improves the fundamental amplitude of the back electromotive force compared with the traditional Halbach array. Gao Fengyang et al. [9] found that the use of partially segmented Halbach arrays can reduce the eddy current loss of the motor, making it have great application potential in high-speed and high-power-density motors. Y. Ni et al. [10] proposed a double-layer Halbach array and analyzed and determined the

optimal magnetic segment radian ratio and magnetization angle of each double-layer array, which showed better electromagnetic performance than the single-layer Halbach array. Bonkil Koo et al. [11] studied the effect of permanent magnet thickness on ring magnets magnetized in a sinusoidal manner and found the optimal permanent magnet thickness. Seok-Myeong Jang et al. [12] used 2D finite element method to study two types of high-speed slotless permanent magnet machines with the rotor eccentricity and discussed the advantages of Halbach array. At present, Halbach segmental magnetization, which is widely used, still causes harmonics in the air gap magnetic density, which will cause vibration and noise of the motor. But the continuously magnetized Halbach array can generate a highly sinusoidal air-gap magnetic density to solve this problem [13].

It can be seen that scholars at home and abroad have extensively studied the application of Halbach arrays with various design structures of the inner rotor permanent magnet motor to optimize the electromagnetic performance of the motor. However, the optimal design of applying it to the outer rotor permanent magnet motor and combining it with other motor structures is still lacking. In this paper, the ring permanent magnet Halbach magnetization is applied to an ERPMM, and auxiliary slots are opened on the stator teeth to further improve the performance of the motor.

2. Models and Principles

2.1. Designs of Motors

The structural diagram of ERPMM is shown in Figure 1 below. The A, B, and C three-phase windings on the motor stator are connected in star form. The windings are energized according to different timings under the rated power to drive the air gap magnetic field to rotate. The permanent magnet magnetization method of the rotor is radial Magnetizing.

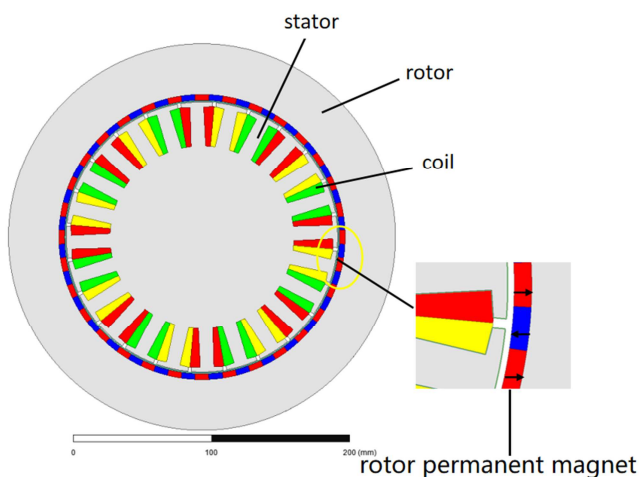


Figure 1. Schematic diagram of ERPMM.

In order to improve the output torque capability of the permanent magnet motor at the rated speed, the permanent magnet is changed to the Halbach magnetization structure

with the advantages of magnetic concentration to form an A-type Halbach external rotor permanent magnet motor (Halbach External rotor permanent magnet motor A, HERPMMA), and slotting the stator teeth to form a B-type Halbach external rotor permanent magnet motor (Halbach External rotor permanent magnet motor B, HERPMMB). The schematic diagrams of HERPMMA and HERPMMB are shown in Figure 2 and Figure 3.

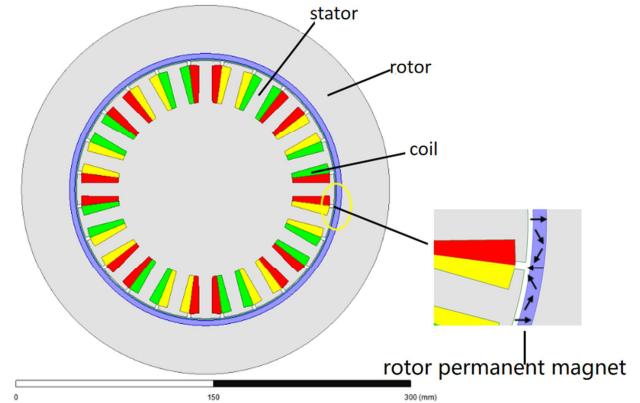


Figure 2. Schematic diagram of HERPMMA.

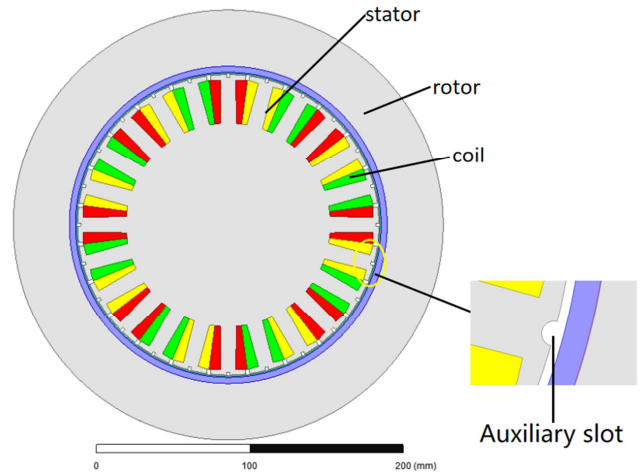


Figure 3. Schematic diagram of HERPMMB.

Compared with ERPMM, HERPMMA and HERPMMB do not change the amount of permanent magnets, but reduce the flux leakage on the basis of the prototype motor ERPMM, and improve the magnetic gathering ability of the motor structure and the utilization rate of permanent magnets. In order to reasonably compare the performance of the operating parameters of the three motor structures, their main design parameters such as rated speed, axial length, inner and outer diameters of the stator and rotor, number of slots, and slot type are all consistent. Compared with HERPMMA, HERPMMB has the same design parameters except for slotting of stator teeth.

2.2. Principle of Motor Operation

The relationship between flux, permeability and potential difference in the motor magnetic circuit is shown below [14]:

$$\varphi_{\delta} = \Lambda_{\delta} \Sigma F \quad (1)$$

$$\varphi_m = B A_m \quad (2)$$

Where Φ_m is the total magnetic flux per pole provided by the permanent magnet to the external magnetic circuit; B is the magnetic induction intensity; A_m is the cross-sectional area (m^2) of magnetic flux per pole of permanent magnet. Φ_{δ} is the air gap flux per pole of permanent magnet; Λ_{δ} is the main permeability of the permanent magnet. ΣF is the sum of the magnetic potential difference of each magnetic circuit and is positively correlated with the magnetic field strength. The relationship is as follows:

$$\varphi_{\sigma} = \varphi_m - \varphi_{\delta} = (\sigma - 1)\varphi \quad (3)$$

Where Φ_{σ} is the leakage flux of ERPMM, σ is the leakage flux coefficient (which is a constant determined by the motor structure and σ is always greater than 1).

$$\sigma = \frac{\varphi_{\delta}}{\varphi_m} = \frac{\int B_{\delta} dS_{\delta}}{\int B_m dS_m} \quad (4)$$

Where: S_{δ} -- integral area of total magnetic circuit;

S_m -- integrated area of main magnetic circuit;

B_{δ} -- magnetic density on the integrated surface of the total magnetic circuit;

B_m -- magnetic density on the integrating surface of the main magnetic circuit.

When the end magnetic leakage is ignored and the motor is assumed to be axially symmetric:

$$\sigma = \frac{\varphi_{\delta}}{\varphi_m} = \frac{\int B_{\delta} \cdot dL_{\delta}}{\int B_m \cdot dL_m} \quad (5)$$

L_{δ} -- total magnetic circuit integral path;

L_m -- total magnetic circuit integrated area.

Therefore, in order to reduce the flux leakage coefficient in the design of the motor structure, it is necessary to increase the proportion of the main flux in the total flux.

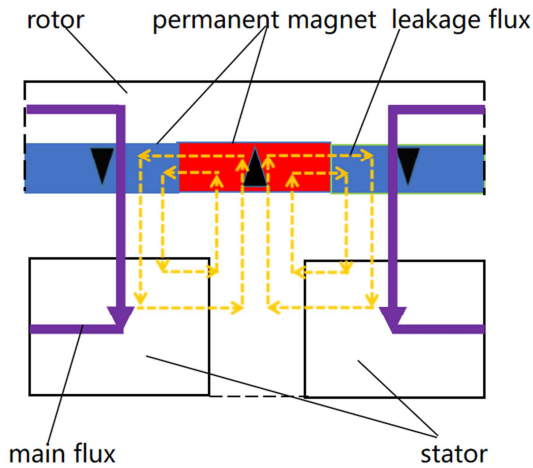
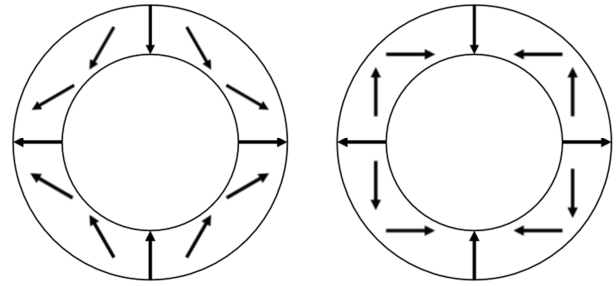


Figure 4. General ERPMM flux model.

The permanent magnet material in ERPMM adopts the traditional radial magnetization, and the serious flux leakage of the magnetic circuit at the stator slot causes the utilization rate of the permanent magnet to be low. As shown in Figure 4, the structure design of ERPMM limits the motor input torque boost and reduces the cost.

The permanent magnets of the rotor are arranged radially inward and radially outward alternately, so that the magnetic flux of the permanent magnet opposite to the position of the stator notch will pass through its adjacent permanent magnets in the opposite direction to form a closed circuit and become a leakage flux. Relative to the permanent magnet at its adjacent position, the permanent magnet leaks part of its own magnetic flux at the permanent magnet resulting in short-circuits. Since this part of the magnetic flux does not participate in the formation of the output torque, the utilization rate of the permanent magnet is low. Changing the magnetization method is an effective way to reduce the leakage flux by gathering the magnetism in the direction of the main flux.

Halbach magnetization can fully tap the potential of the magnetic steel, so that the waveform sine of the air gap magnetic field and the back electromotive force is better. Not only is it beneficial to give full play to the advantages of magnetic concentration, but it is also beneficial to reduce the torque ripple under load conditions and the cogging torque under no-load conditions. There are two types of Halbach magnetization: block type and integral type. As shown in Figure 5, the length of the ERPMM permanent magnet is relatively small. This paper mainly focuses on the integral type.



(a) Outward magnetization

(b) Inward magnetization

Figure 5. Two Halbach magnet types.

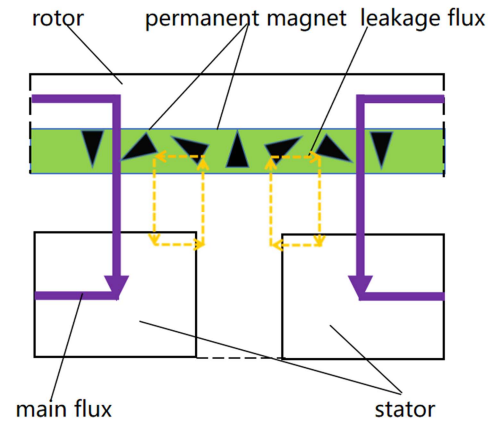


Figure 6. General ERPMM flux model.

Integral Halbach magnetization is divided into outward magnetization and inward magnetization, which are suitable for inner rotor motors and outer rotor motors respectively. As shown in Figure 6, the Halbach-magnetized ERPMM with integral outward magnetic concentration can effectively reduce the leakage flux of the permanent magnet at the notch.

3. Results Analysis

The ERPMM design adopts the outer rotor structure, and the specific design parameters are shown in Table 1. The main design parameters of the other two motors HERPMMMA and HERPMMB in the article are also consistent with ERPMM.

Table 1. Parameters of the ERPMM.

Parameters	
Rated speed (r/min)	1500
Stator outer diameter (mm)	199
Rotor inner diameter (mm)	202
Rotor outer diameter (mm)	310
Permanent magnet thickness (mm)	4
Axial length (mm)	156
Air gap length (mm)	1.5
Number of pole pairs of permanent magnet	32
Number of stator slots	24
Coil Turns	30
Permanent magnet material	N45SH
Stator and rotor silicon steel sheet material	DW465
Pole structure	Surface mount

3.1. Analysis of No-Load Running Parameters

The magnetic flux density when the motor is running at rated speed under no-load conditions is shown in Figure 7. The magnetic flux density in the stator teeth of the three motors increases sequentially. Firstly, the flow of the magnetic flux in the permanent magnet to the direction of the main magnetic flux is strengthened due to the full use of the advantages of the magnetic concentration of the Halbach magnetization. On this basis, the motor structure is optimized by slotting the stator teeth, which further enhances the magnetic field concentration effect.

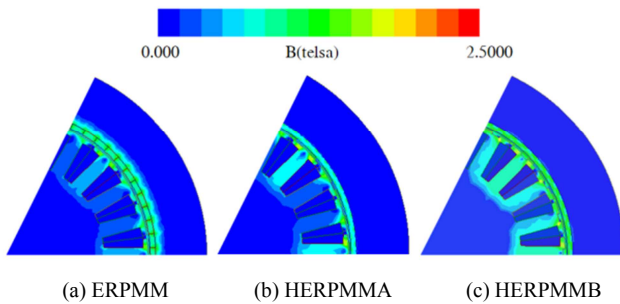


Figure 7. Flux density distribution of three kinds of motor.

On this basis, the motor structure is optimized by slotting the stator teeth, which further enhances the magnetic field concentration effect. In the magnetic flux density of the motor structure, the radial flux density of the air gap is an important parameter to characterize the performance of the

motor, which determines the power density of the motor to a large extent. The radial magnetic flux density distribution at the air gap positions of the three motors are shown in Figure 8. The maximum magnetic flux densities at the center of the stator teeth of ERPMM, HERPMMMA and HERPMMB are 0.94T, 1.21T and 1.24T respectively. Comparing the air gap radial flux density of the three motors, it is found that the Halbach magnetization method can significantly enhance the radial air gap flux density, but the effect of slotting the stator teeth on the enhancement of the air gap flux density is limited.

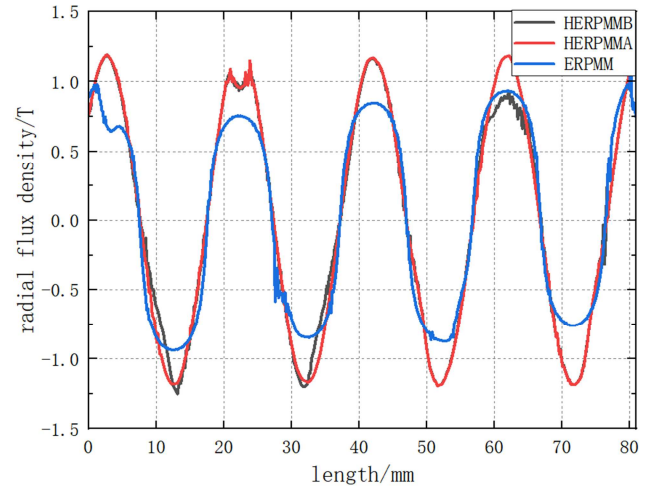


Figure 8. Radial air gap flux density distribution of three kinds of motor.

The enhancement of the air gap flux density under no-load conditions will increase the back electromotive force of the motor. Taking the A-phase winding as an example, the back electromotive force of the three motors under no-load operation is shown in Figure 9. The maximum value of back electromotive force amplitude of ERPMM, HERPMMMA, HERPMMB is 56.8V, 69.0V, 79.6V respectively. Through comparative analysis, it is found that HERPMMB has the largest induce voltage amplitude, while ERPMM has the smallest induce voltage amplitude.

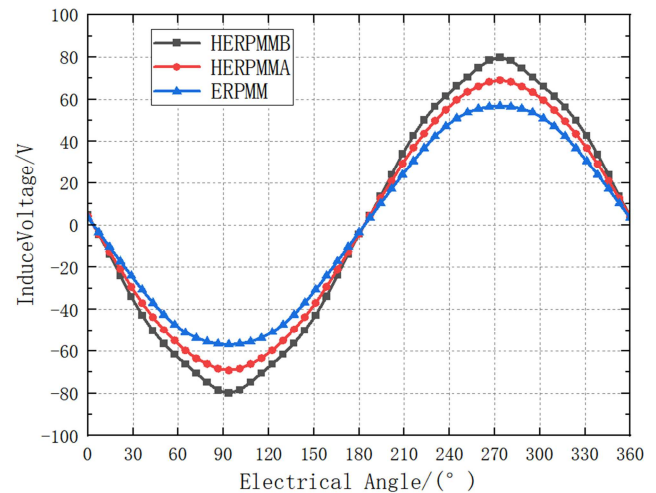


Figure 9. No-load BEMF of three kinds of motor.

The stator cogging torque generated by the interaction between stator cogging and permanent magnet in no-load state will have an adverse effect on the torque stability and speed stability of the motor. Cogging torque is defined as follows [15]:

$$T_{\text{cog}}(\alpha) = -\frac{\partial W}{\partial \alpha} \quad (6)$$

Where, W is the magnetic co-energy, assuming that W in the rotor core and permanent magnet is stable and unchanged, W in the air gap is:

$$W_{\text{gap}} = \frac{1}{2\mu_0} \int_v G^2(\theta) B^2(\theta, \alpha) dv \quad (7)$$

Where, μ is the vacuum relative permeability, and $G^2(\theta)$ is the air gap relative permeability function considering the slotting effect. $B^2(\theta, \alpha)$ is the magnetic density of no-load air gap. $G^2(\theta)$, $B^2(\theta, \alpha)$ can be expressed as follows:

$$G^2(\theta) = G_{\alpha 0} + \sum_{k=1}^{\infty} G_{\alpha k N_s} \cos(K N_s \theta) \quad (8)$$

$$B(\theta, \alpha) = \mu_0 \frac{F(\theta)}{h_c + \delta(\theta, \alpha)} \quad (9)$$

Where N_s is the number of stator slots, $G_{\alpha 0}$ and $G_{\alpha k N_s}$ are Fourier coefficients; $F(\theta)$, h_c , $\delta(\theta, \alpha)$ are the distribution of air gap magnetomotive force, the thickness of permanent magnet and the length of effective air gap along the circumference respectively.

Under no-load conditions, the cogging torques of the three motor structures are shown in Figure 10. It can be seen from Figure 10 that the peak cogging torque of HERPMMMA and HERPMMB is only 7.94% and 21.36% of that of ERPMM. The reason is that the Halbach magnetization makes the air gap flux density more sinusoidal and reduces the harmonic content. Slotting increases the number of stator slots, which will have a negative effect on weakening the cogging torque, so the cogging torque of HERPMMB is 1.69 times higher than that of HERPMMMA.

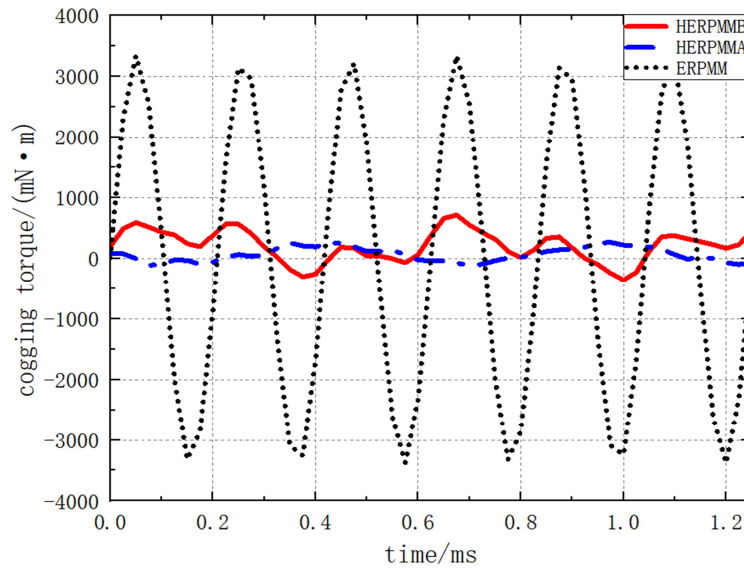


Figure 10. Cogging torque of three kinds of motor.

3.2. Analysis of Load Operating Parameters

Under load conditions, adding a current with a phase difference of 120° and an effective value of 10A to the A, B, and C three-phase windings of the motor, and setting the rotor speed of the motor to 900r/min. In the case of keeping other structural parameters of the motor unchanged, an auxiliary slot is opened in the center of the stator teeth of HERPMMMA, as shown in Figure 11 below.

The depth H and width W of the rectangular slot on the stator teeth and the radius R of the circular slot will affect the load torque. In order to further characterize the influence of the three parameters on the load torque, the depth H and width W of the rectangular slot and the radius R of the circular slot is analyzed by parametric simulation.

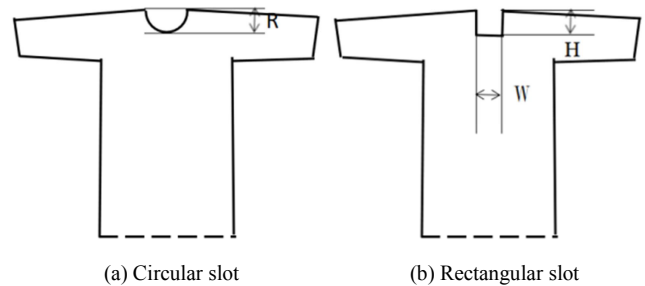


Figure 11. Auxiliary slots for stator teeth.

Figure 12 shows the load torque of the motor with rectangular slots under different H and W on the stator teeth, and Figure 13 shows the load torque of the motor with

circular slots under different R .

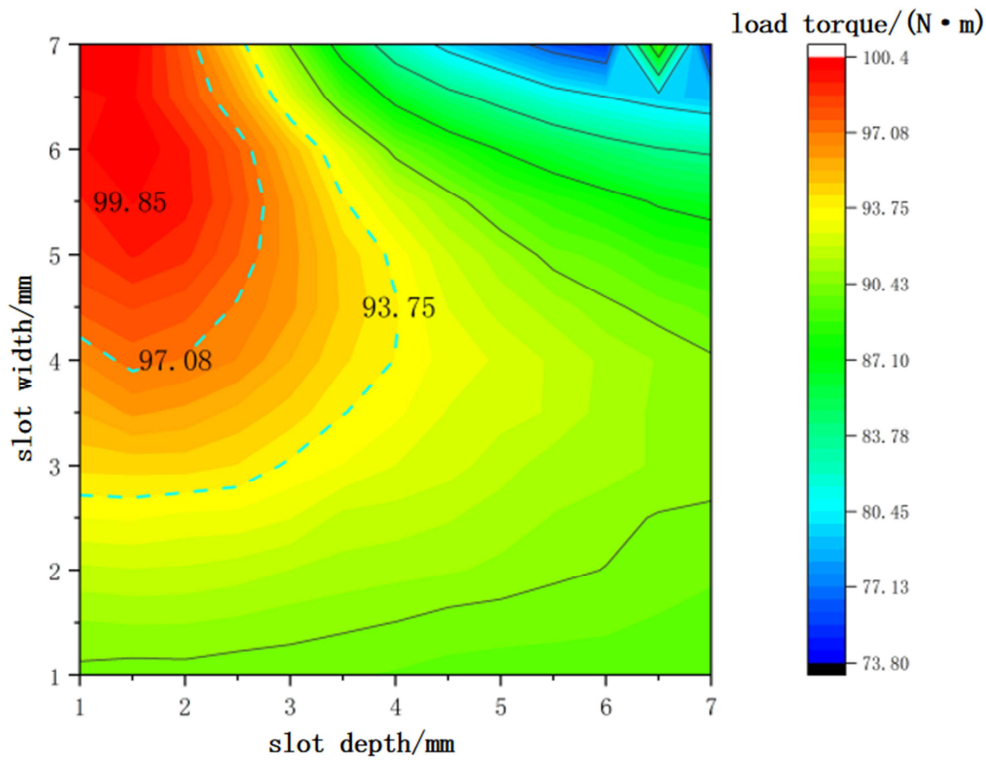


Figure 12. Load torque under different H and W .

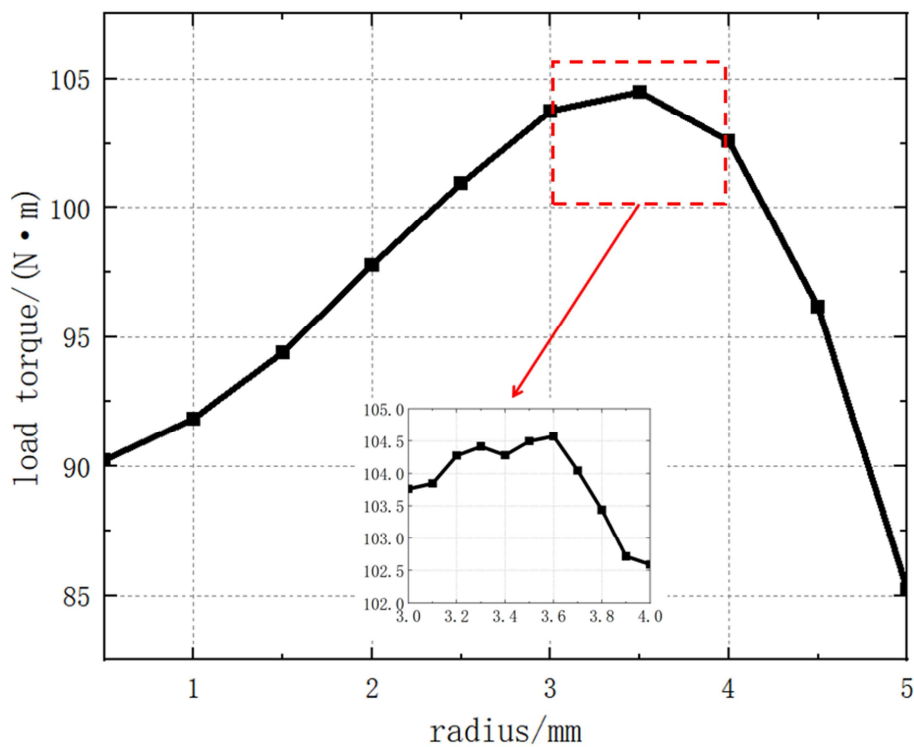


Figure 13. Load torque under different R .

The results are compared and analyzed. When the depth of the rectangular slot is 1.5mm and the width is 5.5mm, the maximum load torque is 99.85N·m. With the increase of the radius of the circular cogging, the load torque firstly increases

and then decreases, and reaches the maximum value 104.57N·m when the radius is 3.5mm. HERPMMB is based on HERPMMMA for structural optimization. The output torque of the three motor structures is shown in Figure 14.

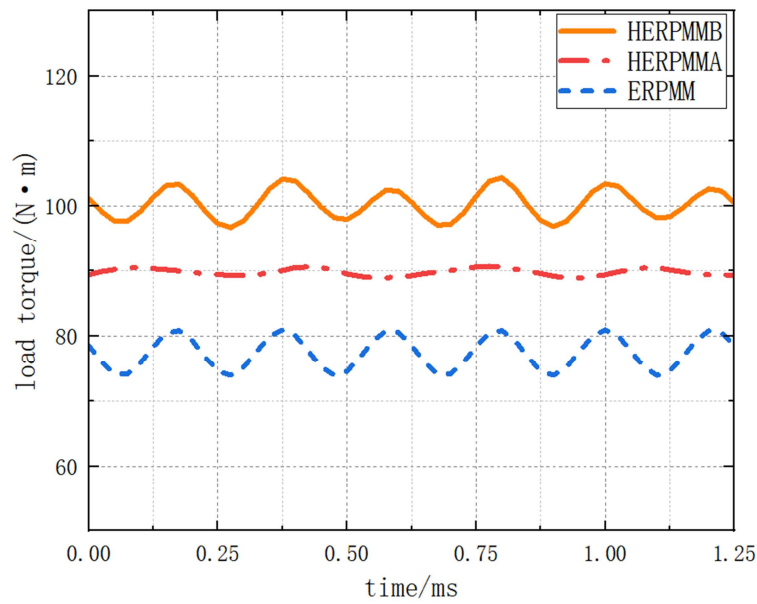


Figure 14. Load torque of three kinds of motors.

The electromagnetic performance comparison of the three motors under no-load and load conditions is shown in Table 2 below.

Table 2. Performance comparison of three kinds of motors.

Parameters	ERPMM	HERPMMA	HERPMMB
Counter electromotive force (V)	56.84	69.03	79.63
Cogging torque (N·m)	3.34	0.27	0.71
output torque (N·m)	73.19	89.75	104.57
Permanent magnet utilization (N·m/mm ³)	1.81E-4	2.22E-4	2.59E-4
Torque ripple/%	12.33	2.23	9.62

Among the three motor structures, compared with ERPMM permanent magnets using radial magnetization, HERPMMA magnetized by Halbach has greatly improved output torque, weakened cogging torque, and improved permanent magnet utilization. On the basis of HERPMMA, the output torque of HERPMMB with auxiliary slots in the stator is improved, and the cogging torque is also increased. The comprehensive performance of the HERPMMB structure is considered to be stronger by comparing various performance parameters.

4. Conclusion

In order to improve the torque performance of the outer rotor permanent magnet motor under no-load and load conditions and to improve the utilization rate of the permanent magnet, this paper applies the Halbach magnetization method and the auxiliary slot design to ERPMM and proposes two new motor optimization structures HERPMMA and HERPMMB. The key variables such as leakage flux, air-gap flux density, and cogging torque of the three motor structures were theoretically analyzed and two-dimensional finite element simulations were carried out. Various operating parameters under different slotting designs in different magnetization methods were explored. Through

the comparative analysis of the simulation results, the following conclusions can be drawn:

- 1) Halbach magnetization fully taps the potential of the magnetic steel, reduces the leakage flux and enhances the air gap flux density of the stator and rotor under the condition of the same permanent magnet size. While giving full play to the advantages of magnetic concentration, the sine of the air gap magnetic density is improved, and the harmonic amplitude of the magnetomotive force is weakened.
- 2) The optimal design of opening auxiliary slots for HERPMMA was carried out, and the parametric analysis was carried out for the two types of slots, and an optimal solution design HERPMMB was proposed considering various performance parameters.
- 3) After the structural design is optimized based on Halbach magnetization, the output torque and permanent magnet utilization of HERPMMB increased by 42.88% and the cogging torque of the motor decreased by 78.63% compared with ERPMM without changing the amount of permanent magnets.

Author Contributions

Conceptualization, Z. R.; methodology, Z. R.; software, Z.

R.; validation, Z. R. and T. L.; formal analysis, Z. R. and T. L.; writing—original draft preparation, Z. R. and T. L.; writing—review and editing, Z. R. and T. L. All authors have read and agreed to the published version of the manuscript.

Acknowledgements

This research received no grant from funding agencies in the public, commercial, or not-for-profits sectors.

References

- [1] A. M. EL-Refaie, "Fractional-Slot Concentrated-Windings Synchronous Permanent Magnet Machines: Opportunities and Challenges," in *IEEE Transactions on Industrial Electronics*, vol. 57, no. 1, pp. 107-121, Jan. 2010.
- [2] J. G. W. West, "DC, induction, reluctance and PM motors for electric vehicles," in *Power Engineering Journal*, vol. 8, no. 2, pp. 77-88, April 1994.
- [3] T. Takahashi, M. Takemoto, S. Ogasawara, W. Hino and K. Takezaki, "Size and Weight Reduction of an In-Wheel Axial-Gap Motor Using Ferrite Permanent Magnets for Electric Commuter Cars," in *IEEE Transactions on Industry Applications*, vol. 53, no. 4, pp. 3927-3935, July-Aug. 2017.
- [4] Yan he, Yang Lei, Zhang Zuo-peng et al., "Experimental Study on Cold State Rod Dropping of Control Rod Drive Mechanism of High Temperature Gas Cooled Reactor," in *Nuclear Science and Engineering* 2015, 35 (03): 479-485. (In Chinese with English abstract).
- [5] T. Tymosch, M. Fischer, V. Ketchedjian, Y. Terao and H. Ohsaki, "Analysis of Superconducting Synchronous Motors With Halbach Array Field Excitation," in *IEEE Transactions on Applied Superconductivity*, vol. 31, no. 2, pp. 1-5, March 2021, Art no. 5200205.
- [6] K. Liu, M. Yin, W. Hua, Z. Ma, M. Lin and Y. Kong, "Design and Analysis of Halbach Ironless Flywheel BLDC Motor/Generators," in *IEEE Transactions on Magnetics*, vol. 54, no. 11, pp. 1-5, Nov. 2018, Art no. 8109305.
- [7] Wang Xiuping, Jiang Shenglong, Qu Chunyu, "Structural optimization design of Halbach array permanent magnet cursor motor," in *Electric Machines and Control*, 2023, 27 (04): 140-147. (In Chinese with English abstract).
- [8] X. Zhang, C. Zhang, J. Yu, P. Du and L. Li, "Analytical Model of Magnetic Field of a Permanent Magnet Synchronous Motor With a Trapezoidal Halbach Permanent Magnet Array," in *IEEE Transactions on Magnetics*, vol. 55, no. 7, pp. 1-5, July 2019, Art no. 8105205.
- [9] Gao Fengyang, Qi Xiaodong, Li Xiaofeng et al., "Analytical calculation and optimization analysis of electromagnetic performance of Halbach partially-segmented permanent magnet synchronous motors with unequal width and thickness," in *Transactions of China Electrotechnical Society* 2022, 37 (06): 1398-1414. (In Chinese with English abstract).
- [10] Y. Ni, X. Jiang, B. Xiao and Q. Wang, "Analytical Modeling and Optimization of Dual-Layer Segmented Halbach Permanent-Magnet Machines," in *IEEE Transactions on Magnetics*, vol. 56, no. 5, pp. 1-11, May 2020, Art no. 8100811.
- [11] B. Koo, J. Kim and K. Nam, "Halbach Array PM Machine Design for High Speed Dynamo Motor," in *IEEE Transactions on Magnetics*, vol. 57, no. 2, pp. 1-5, Feb. 2021, Art no. 8202105.
- [12] Z. Q. Zhu, Z. P. Xia and D. Howe, "Comparison of Halbach magnetised brushless machines having discrete magnet segments or single ring magnet," 2002 *IEEE International Magnetism Conference (INTERMAG)*, Amsterdam, Netherlands, 2002.
- [13] S.-M. Jang, Sung-Ho Lee, Han-Wook Cho and Sung-Kook Cho, "Analysis of unbalanced force for high-speed slotless permanent magnet machine with Halbach array," in *IEEE Transactions on Magnetics*, vol. 39, no. 5, pp. 3265-3267, Sept. 2003.
- [14] Wang Peixin, Hua Wei, Hu Mingjin et al., "Design of performance analysis of Flux-switching permanent magnet machine with cos-charactering rotor," in *Proceedings of the CSEE* 2022, 42 (22): 8372-8382.. (In Chinese with English abstract).
- [15] HWANG S M, EOM J B, HWANG G B, et al., "Cogging torque and acoustic noise reduction motors permanent magnet by teeth pairing," in *IEEE Transactions on Magnetics*, 2000, 36 (5): 3144-3146.